Applied Clay Science 238 (2023) 106947

Contents lists available at ScienceDirect

Applied Clay Science

journal homepage: www.elsevier.com/locate/clay

Research Paper

Oil-in-oil Pickering emulsions stabilized by shigaite-like layered double hydroxide particles

Lilian Fernanda Martins do Amaral [a], Gabriela Siegel Aires [a], Fernando Wypych [a,*], Rilton Alves de Freitas [b,*]

[a] Department of Chemistry, Federal University of Paraná, Caixa Postal 19032, Centro Politécnico, Jardim das Américas, 81531-980 Curitiba, PR, Brazil
[b] Department of Pharmacy, Federal University of Paraná, Caixa Postal 19005, Setor de Ciências da Saúde, Jardim Botânico, 80210-170 Curitiba, PR, Brazil

ARTICLE INFO

Keywords:
Oil-in-oil emulsion
Pickering emulsion
Layered double hydroxides

ABSTRACT

In this work, we report the preparation of simple oil-in-oil emulsions using layered nanoparticles as stabilizers at the interface between silicone and castor oil. Layered double hydroxides with a shigaite-like structure presenting an ideal composition of $[Mn_6Al_3(OH)_{18}][(SO_4)_2Na]\cdot 12H_2O$ (S-Na/SO_4) were prepared by co-precipitation with increasing pH, followed by particle surface grafting with octhadecyltrimethoxysilane (S-OTMS) in an apolar medium. The powder XRD, SEM, TEM, and specific surface area (BET) techniques showed that the structure and morphology of silane-grafted S-Na/SO_4 remained practically unchanged. FTIR, EDS and ICP-OES analyses indicated that the silanes were successfully grafted onto the S-Na/SO_4 surface. In addition, to maintaining their structure and morphology, these functionalized materials showed good performance in controlling the hydrophobicity of the surface for application in oil-in-oil emulsions, improving their compatibility for the dispersion in non-polar liquids.

1. Introduction

Oil-in-oil (o/o) emulsions are water-free formulations that are rarely reported in the literature (Thompson et al., 2015; Binks and Tyowua, 2016; Tyowua et al., 2017; Zia et al., 2020) due to the lack of simple stabilization methods. However, these emulsions can offer advantages over traditional oil-in-water (o/w) emulsions, mainly due to the absence of water, such as in moisture-sensitive substances and controlled release processes of drugs that are unstable in water (Klapper et al., 2008; Atanase and Riess, 2011; Tawfeek et al., 2014; Mei et al., 2018).

As is well known, the interface between two immiscible liquids, in terms of free surface energy, is thermodynamically unfavorable, and this energy can be minimized by reducing the interfacial tension with a suitable stabilizer, usually a surfactant (Tadros, 2013; Sharma et al., 2015). However, the emulsions are normally in a metastable state, associated with repulsive and/or steric hindrance kinetic stability. Oil-in-oil (o/o) emulsions can also be stabilized by other interfacial stabilizers like surfactant molecules, such as block copolymers and solid particles, the latter being less reported (Tawfeek et al., 2014; Rodier et al., 2017), and can spontaneously accumulate at the interface of the oil droplets. Unlike surfactants, these particles do not need to be amphiphilic, but have to be partially wetted by both phases (Rodier et al., 2017). This criterion has been met by some inorganic and organic particles, such as silica with different hydrophobicity (Tyowua et al., 2017; Dyab et al., 2018; Rozynek et al., 2018), a mixture of graphene oxide nanosheets and primary alkylamines (Rodier et al., 2017), a mixture of kaolinite and Noigen-RN10 (Tawfeek et al., 2014), hydrophobic bentonite (Vartanian and Brook, 1969), and magnetite (Bielas and Józefczak, 2020) in classical emulsions.

Among the particles to stabilize Pickering emulsions, clay minerals, synthetic or natural, are well described in literature (Yu et al., 2021; Wang et al., 2022; Lisuzzo et al., 2022). Here, shigaite-like layered double hydroxides (LDH) have shown great potential (Amaral et al., 2020, 2021) as Pickering particle. This hydrophilic LDH occurs in the form of a mineral ($[Mn_6Al_3(OH)_{18}][(SO_4)_2Na]\cdot 12H_2O$) (Cooper and Hawthorne, 1996), and is easily synthesized by co-precipitation. It can also exchange cations, anions, and even both simultaneously (Sotiles et al., 2019, 2019a, 2019b; Sotiles and Wypych, 2019, 2020; Gomez et al., 2020), unlike traditional LDHs, which can only exchange anions (Crepaldi et al., 1999; Vaccari, 2002; Wypych and Satyanarayana, 2004).

The formation of modified LDH surfaces was previously explored to

* Corresponding authors.
E-mail addresses: wypych@ufpr.br (F. Wypych), rilton@ufpr.br (R.A. de Freitas).

https://doi.org/10.1016/j.clay.2023.106947
Received 3 December 2022; Received in revised form 7 March 2023; Accepted 30 March 2023
Available online 6 April 2023

obtain hydrophobic characteristics (Park et al., 2005; Wypych et al., 2005; Chen et al., 2014, 2020; Tao et al., 2014; Guo et al., 2016). These interactions can occur through the process of silylation (silane grafting) of chemical bonds via the reaction of silane with the hydroxyl groups on the LDH surface, enabling precise control over the surface components and porous characteristics for several applications (Wypych et al., 2005; Wang et al., 2012; Xu et al., 2016; Zhang et al., 2017). Here, the objective was to maintain particle properties such as morphology, surface area and porosity after silane modification, improving their compatibility with the oil phases.

Thus, the ease of synthesis and structural modification, as well as the platelet-like morphology, make shigaite-like LDHs excellent candidates for oil-in-oil Pickering emulsion stabilization, as evaluated in this work. To extend the applications of shigaite-like LDHs, the hydrophobization of the layered particles was performed using octadecyltrimethoxysilane (OTMS - $C_{21}H_{46}O_3Si$), and the two particles were compared in castor oil and silicone oil formulations.

2. Materials and methods

2.1. Materials

All chemicals were of reagent grade and used without further treatment. All solutions were prepared using silicone oil (Êxodo Científica - $\rho = 0.96$ g cm^{-3}, 25 °C; $\gamma = 20.23$ mN m^{-1}) and castor oil (Farmanil Quima - $\rho = 0.96$ g cm^{-3}, 25 °C; $\gamma = 36.72$ mN m^{-1}). Neat and grafted layered double hydroxides were prepared by using $Al_2(SO_4)_3 16H_2O$ (Alphatec, 98%) $MnSO_4$ (Alphatec, 98%), Na_2SO_4 (Neon, 99.9%), NaOH (Neon, 97%), toluene (Synth, 99.5%), OTMS - $C_{21}H_{46}O_3Si$ (Sigma-Aldrich, 90%) and ultrapure water (18.2 MΩ cm, $\rho = 0.997$ g cm^{-3} at 25 °C, Milli-Q system - Millipore).

2.2. Synthesis of S-Na/SO_4 nanoparticles

The layered double hydroxide with the shigaite-like structure (S-Na/SO_4) and ideal formula $[Mn_{0.666}Al_{0.333}(OH)_2][Na_{0.111}(H_2O)_{0.666}(SO_4)_{0.222}]0.666H_2O$ was synthesized by co-precipitation with increasing pH, as previously reported (Sotiles et al., 2019a). Solutions of $MnSO_4$ (26.13 mmol), $Al_2(SO_4)_3$ (6.53 mmol) and Na_2SO_4 (2.18 mmol) were dissolved in 100 mL of ultrapure water, with a molar ratio of 6:3:1, and slowly titrated with a solution of NaOH (0.5 mol L^{-1}) in a glass reactor, until reaching pH 9.05.

The precipitation was conducted at 90 °C, and to avoid contamination of carbonate, the reaction was performed with a continuous flow of N_2. After precipitation, the materials were kept at 90 °C for 120 h, centrifuged at 4000 rpm (centrifugal force of 2125 G, 5 min), washed three times with ultrapure water and dried at 40 °C.

2.3. Synthesis of silane-modified S-Na/SO_4 nanoparticles

According to an adaptation of the procedure previously described (Guo et al., 2016), approximately 1 g of S-Na/SO_4 was dispersed in 25 mL of toluene, and then 2.5 mmol of OTMS was added dropwise to the mixture and kept in an inert N_2 atmosphere. After stirring for 24 h at 80 °C, the resulting material was washed three times with toluene, centrifuged at 4000 rpm (centrifugal force of 2125 G, 5 min), and then dried at 80 °C.

Oriented X-ray diffraction (XRD) patterns were obtained after placing the last washing slurry on glass holders and drying at room temperature. The measurements were carried out with a Shimadzu diffractometer (model XRD-6000) with CuK_α radiation source of $\lambda = 1.5418$ Å, current of 30 mA, a voltage of 40 kV, time of 2° min^{-1} and step of 0.02°.

Fourier-transform infrared (FTIR) spectra were obtained in transmittance mode using KBr pellets containing about 1 wt% of the sample. The pellets were produced at pressure of 7 tons for 5 min (hydraulic press, Shimadzu SSP-10A) and analyzed in a Bruker Vertex 70 spectrophotometer. The spectra were collected from 400 to 4000 cm^{-1}, with 32 scans and resolution of 2 cm^{-1}.

Scanning electron microscopy (SEM) and energy dispersive spectroscopy (EDS) measurements were performed with a Tescan Vega3LMU microscope with AZ Tech software. Sample dispersions were deposited on copper tapes and after EDS analysis, they were coated with a thin gold layer for image acquisition.

Transmission electron microscopy (TEM) analyses were performed using a JEOL JEM 1200EX-II microscope operating at 120 kV. Sample dispersions were deposited on 2 mm copper grids, coated with amorphous carbon and dried at room temperature.

Silicon was quantified in the S-OTMS sample using an ICP-OES spectrometer (Thermo Scientific-model iCAP 6500), and the data were treated with the ThermoiTeVa Analyst software, version 1.2.0.30. The samples were dissolved in a solution containing 1.0% HNO_3/H_2SO_4 (v/v) and analyzed in duplicate.

Surface area analysis was performed by Brunauer-Emmet-Teller (BET). adsorption/desorption of N_2 isotherms using a Quantachrome NOVA-2000e analyzer at −196 °C, after degassing the samples at 110 °C.

2.4. Preparation and characterization of emulsions

The oil-in-oil emulsions were prepared by dispersing 0.1, 0.25, 0.50, 0.75 or 1.0 wt% of S-Na/SO_4 or S-OTMS particles in different silicone oil fractions ($\Phi_s = 0.3, 0.5, 0.7$), followed by inclusion of castor oil. These mixtures were subjected to ultrasound treatment using a probe (Sonics Vibra Cell; SM0220, Misonix) for 1 min at 40% amplitude (750 W and 20 kHz frequency) and kept at a constant temperature (22 °C). Then, the macroscopic study of the emulsions was performed by obtaining images at specified time intervals since preparation. The emulsion preparation was evaluated for 30 days. In addition to this assessment, the height of the emulsified volume was digitally measured using the Image J software to compare each tube to the total volume before shaking.

Microscopic images of the emulsions were obtained using an optical microscope (Zeiss Vert.A1). Images were acquired at 200× magnification. For this, the emulsions were placed on a coverslip for microscopic analysis. The droplet diameter was measured 24 h after preparation and all images obtained were processed using the Image J software.

Confocal microscopic images of the emulsions were obtained using a Nikon laser confocal microscope (model AR1+) at 200× and 600× magnification. For this analysis, the particles were stained with rhodamine B (10 ppm, excitation of red fluorescent particles at 563 nm, and emission at 595 nm). In contrast, the castor oil phase was stained with Nile blue (10 ppm, excitation of blue fluorescence at 641 nm and emission at 700 nm). Twelve shots were superimposed using the NIS program's large image mode, combining the 12 images to form a wide frame (4429 × 2253 pixels). The type of emulsion (silicone-in-castor or castor-in-silicone) was analyzed 24 h after preparation and all images obtained were processed using Image J.

Apparent contact angle analyses were performed with a DataPhysics OCA 15 Plus tensiometer using the sessile drop method. Sample pellets were produced at 5 tons for 5 min (hydraulic press, Carver model C, USA). Then, a droplet of oil (2 μL) was placed on the surface, and the pellet-oil-air contact angle was measured. To determine the three-phase contact angle, pellets-silicone-castor (2 μL of silicone oil was inserted under the pellets submerged in the castor oil) was measured. All measurements were obtained at 22 °C using a Hamilton syringe (Bonaduz, Switzerland) in triplicate. The contact angle was determined using the SCA 20 Data Physics software (Filderstadt, Germany).

2.5. Rheological properties

The rheological studies were performed using a TA Instruments HR-10 rheometer equipped with cone geometry (40 mm in diameter and

350 mm gap). Measurements were carried out at a constant temperature of 25 °C, controlled by a thermostatic bath. Oscillatory stress amplitude sweeps were performed from a stress amplitude (τ) of 0.01 Pa to 200 Pa at a frequency of 1 Hz, where the elastic modulus (G′) and viscous modulus (G″) vs. stress amplitude were recorded. Oscillatory frequency sweeps were obtained from a frequency range of 10 to 0.01 Hz at 0.01 Pa (within the linear viscoelastic regime of all tested emulsions).

3. Results and discussion

3.1. Silane modified S-Na/SO_4 characterization

The X-ray diffraction patterns of S-Na/SO_4 and S-OTMS (Fig. 1a) revealed a series of basal peaks typical of layered compounds, where the basal distances were calculated using the third basal peak as 11.03 Å. There was no difference in the XRD patterns of both samples, indicating that the grafting process occurred at the surface of the particles, not between the layers. The basal distances were compatible with the previous results of Sotiles et al. (2019a), who previously synthesized S-Na/SO_4 particles.

The FTIR spectra (Fig. 1B) showed bands for S-Na/SO_4 and S-OTMS in the regions 1146, 1105, 954 and 616 cm^{-1} assigned to typical S-O vibrations. The ν_1 bands observed at 954 cm^{-1} and ν_4 at 616 cm^{-1} were attributed to S-O vibrations of sulfate present in a distorted tetrahedral environment interacting with water molecules, alkali cations and positively charged layers (Sotiles et al., 2019a). Absorption bands attributed to the metal-oxygen (M-O) were observed at 767, 535 and 424 cm^{-1}, and broad bands attributed to O-H vibrations from the lattice and adsorbed/intercalated water molecules were observed at 3428 cm^{-1}. The band at 1639 cm^{-1} was attributed to water molecule bending vibration.

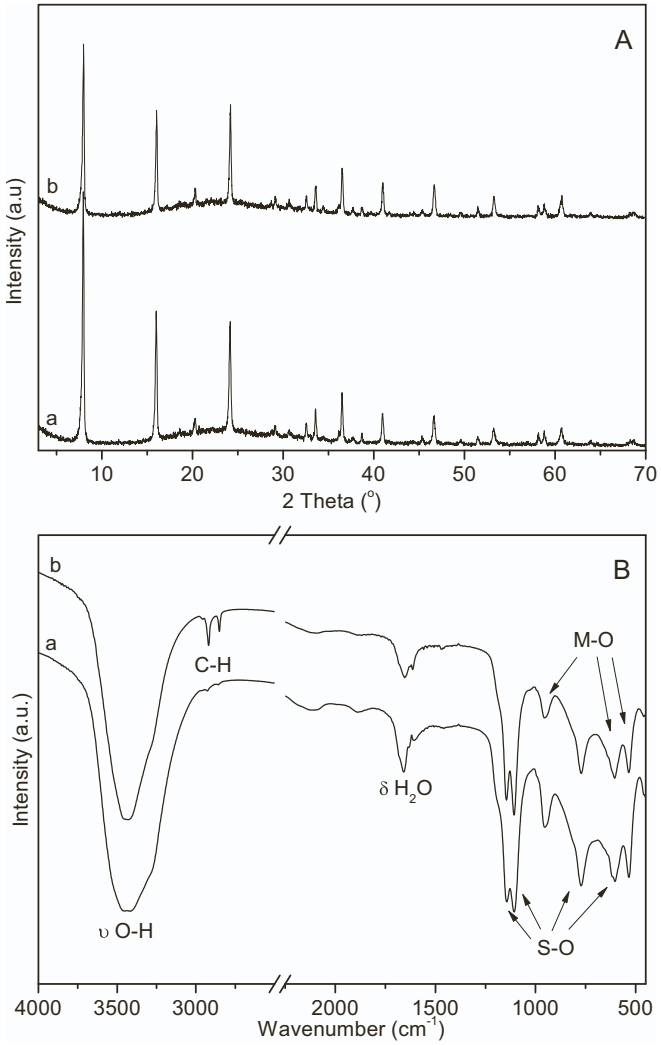

Fig. 1. XRD patterns (A) and FTIR spectra (B) of S-Na/SO_4 (a) and S-OTMS (b).

As indicative of chemical modification on S-OTMS FTIR spectra was observed the presence of bands at 2957, 2920 and 2851 cm^{-1}, attributed to C-H stretching vibrations of the OTMS moieties grafted to the LDH particles, suggesting chemical modifications. At lower wavenumbers, bands in the region of 1145–1107 cm^{-1} were related to additional bands of Si-O-Si and SiO-C stretching mode vibrations (Carrasco et al., 2020), occurring at the same position as the typical S-O vibrations, limiting other FTIR attribution due to OTMS modification. To obtain more information about silane modification, ICP-OES analyses were performed and S-Na/SO_4 value did not indicate the presence of silicon as expected, while S-OTMS showed 4.75 wt% of silicon.

SEM images of S-OTMS particles (Fig. 2a) indicated the presence of platelet-like particles less than 1 μm in diameter with hexagonal morphology and nanometric thicknesses, typical of LDH.

Despite the magnetic stirring for 5 days for grafting of the silanol group, the morphology of the materials did not change. The particles had preserved edges, as observed by the TEM image (Fig. 2b). BET analyses (Fig. S2) showed a small reduction in the surface area (from 21.56 m^2/g in S-Na/SO_4 to 14.81 m^2/g in S-OTMS), indicating the reduction of the area of the basal planes to adsorb N_2, due to the grafting of the organic moieties.

The presence of the silicon from the silanol group in S-OTMS and carbon from the organic moiety were attested by EDS (Fig. 2c), as was the case of the elements expected in the inorganic matrix (Mn, Al, S, Na, O). Furthermore, mapping the surfaces of the samples (Fig. 2d) revealed that all elements were homogeneously distributed throughout the samples at the indicated resolution.

3.2. Characterization of Pickering emulsions

A series of emulsions were prepared to contain a silicone oil fraction ranging from 0.3 to 0.7 in castor oil with increasing concentrations of particles previously dispersed in the silicone phase. S-Na/SO_4 particles were used in previous works by our research group (Amaral et al., 2021) to efficiently stabilize oil-in-water emulsions and were used here as starting materials for the chemical modification of the surface. The color differences of the tubes prepared with and without particles were noticeable. The particles were brown, and when increasing the content of these particles in the formulation, a dark-brown color was observed (Fig. 3). To investigate the long-term stability of the emulsions, they were evaluated for up to 30 days (Fig. 3).

The mixture of oils, free of particles, had no complete phase separation after 30 days due to self-emulsification, observed for a small volume fraction when compared to the emulsions prepared with S-Na/SO_4 and S-OTMS particles. This behavior was associated with the low surface tension between the oily phases. After adding particle to the systems, the emulsions containing S-Na/SO_4 particles were considered macroscopically stable, with complete emulsification at the highest particle concentration (1.00 wt%). On the other hand, emulsions containing S-OTMS particles in fractional volumes with respect to S-Na/SO_4 had smaller droplets at the top, a more emulsified portion in the middle of the tube, and dispersed particles at the bottom of the tube, dispersed in the oil with greatest affinity (silicone oil). This effect was noticed in all formulations with different particle contents present.

The type of emulsion obtained with solid particles depends on how these particles adsorb onto the liquid interface. In this case, the emulsions prepared were all oil-in-oil types, with the continuous phase being castor oil and the dispersed phase being silicone oil. The degree of particles' wettability was given by the three-phase contact angle between the particles and the oil (Fig. 4).

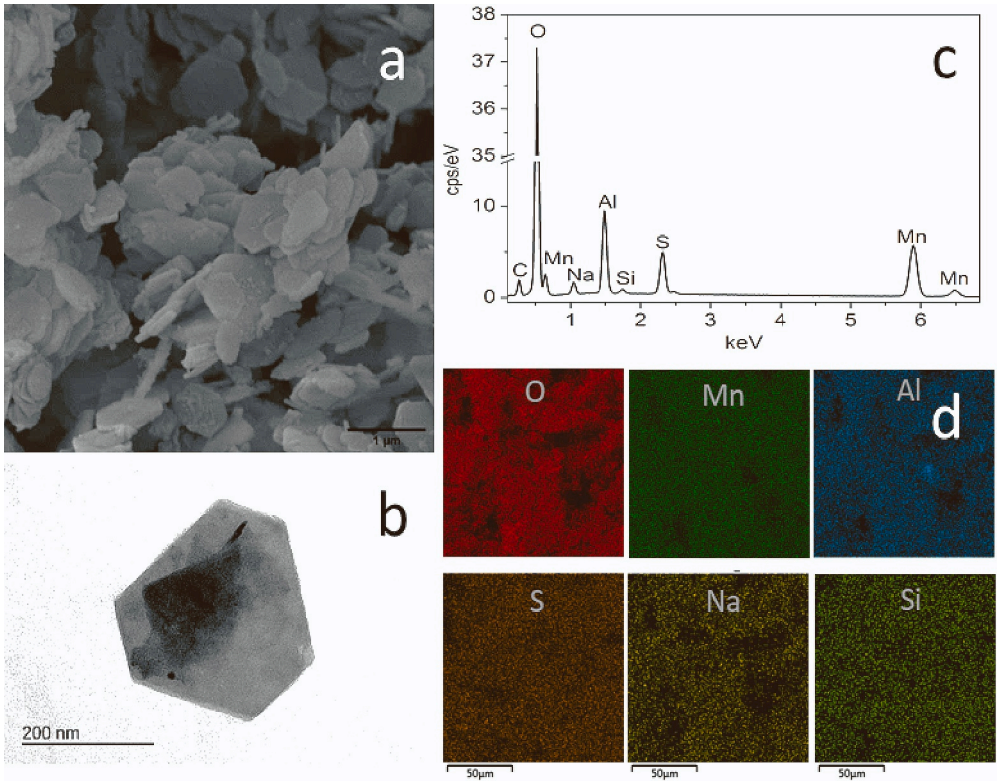

Fig. 2. SEM (scale bar of 1 µm) (a) and TEM image of a single crystal (scale bar of 200 nm) (b), EDS spectra (c) and the corresponding element mappings (scale bar of 50 µm) (d) of S-OTMS particles.

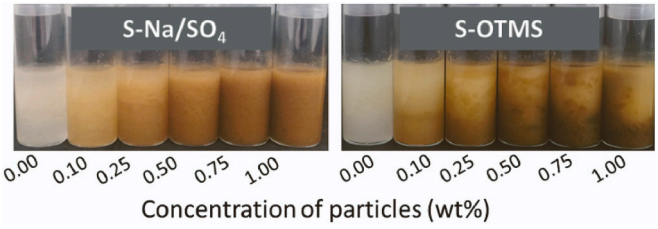

Fig. 3. Photographs of the vessels after 30 days obtained by shaking equal volumes of castor oil and silicone oil with particles ranging from 0.10 to 1.00 wt %. Emulsions containing silicone oil ($\Phi_S = 0.5$).

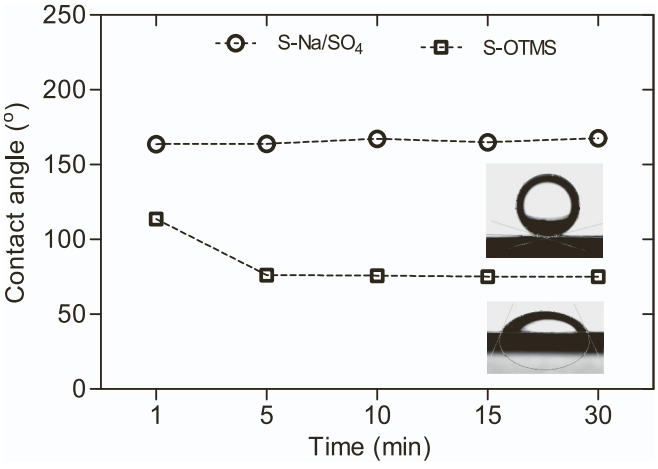

Fig. 4. Evaluation of the three-phase contact angle of emulsions containing a drop of silicone oil in a layer of particles, using castor oil as continuous phase.

The Finkle rule (Finkle et al., 1923) states that stabilization in not possible if the particle is not wetted by both phases, and that the phase that preferentially wets the particles will act as the continuous phase. This behavior was validated with the lamellar particles: the hydrophilic phase (S-Na/SO_4) formed an angle of 43.6° and the hydrophobic phase (S-OTMS) formed a contact angle of 90.3°, as presented in Table S1.

In the oil-in-oil system, castor oil contained a higher amount of ricinoleic acid, a naturally occurring fatty acid that has a hydroxyl at its twelfth carbon. This hydroxyl facilitates its interaction with S-Na/SO_4 particles, while silicone oil contains a linear chain of repeating units of poly(methylsiloxane) [-Si$(CH_3)_2$O-]$_n$ with side groups that interact more easily with the S-OTMS particles. Thus, the modified particles projected more into the silicon phase over time (chosen for particle dispersion) with an initial three-phase angle of 112° and a final one of 77°, suggesting some kinetic aspects associated with the wettability measured.

In turn, the S-Na/SO_4 particles formed an angle of 162°, indicating that both particles, when in contact with both liquids, initially projected more towards the castor oil phase, leading to the formation of a silicone-in-castor emulsion. These differences in the contact angle promoted macroscopic differences in the emulsions formed (Fig. 3), and the affinity of S-OTMS for the silicone phase stood out, in which most of the particles were dispersed in the silicone phase (bottom phase of the tube). The hydrophobization reduced the polarity of the S-OTMS particles, as ideally desired for stabilization of oil-in-oil type emulsions.

Rodier et al. (2017) described the modification of graphene oxide (GO) particles with five different alkylamines to stabilize oil-in-oil emulsions. After functionalizing both surfaces and the edges of GO nanosheets, stable emulsions of DMF-octane and acetonitrile-octane were obtained. Binks and Tyowua (2016) evaluated the hydrophobization of silica particles to stabilize emulsions with different vegetable oils and silicone oil with different viscosities using modified silica particles. They observed a phase inversion in emulsions containing equal volumes of the two oils, from silicone in vegetable (S/*V*) to vegetable in silicone (V/S), when the hydrophobicity of the particles

increased. The values in the three-phase contact angles (silica-sunflower oil-silicone) decreased as the silica hydrophobicity increased, 150° with hydrophilic particles and 44° with hydrophobic ones.

Based on the contact angles (θ) of water, silicone oil and castor oil with the S-Na/SO_4 and S-OTMS particles surfaces, was possible to determine the solid surface free energy (γ_s) and both solid polar (γ_s^p) and solid dispersive (γ_s^d) components. The liquids surface tension (γ_L) and the liquids components polar (γ_L^p) and dispersive (γ_L^d) were found in literature using similar liquid compositions (Table S1).

To obtain γ_s, γ_s^d and γ_s^p was used the Owens, Wendt, Rabel and Kaelble (OWRK) method (Eq. (1)) (Owens and Wendt, 1969). The interactions between solid and liquid are defined as polar (p) and dispersive (d) interactions. The γ_s is the sum of the two parts, ($\gamma_s^p + \gamma_s^d$), where the polar interactions are associated to permanent dipole or Keesom forces, associated to polar interactions. The dispersive components (London forces) are weak forces associated to induced and temporary dipole interactions.

$$\frac{\gamma_L(1+cos\theta)}{2\sqrt{\gamma_L^d}} = \sqrt{\gamma_s^p}\sqrt{\frac{\gamma_L^p}{\gamma_L^d}} + \sqrt{\gamma_s^d} \quad (1)$$

Our results demonstrated, by OWRK method (Fig. S1), that S-Na/SO_4 particles presented a γ_s of 53.42 mJ/m^2; the dispersive component of γ_s^d= 18.10 mJ/m^2 and a polar component of γ_s^p = 35.35 mJ/m^2. As observed the polar component is ~3 times the dispersive one, indicating a more polar surface. S-OTMS particles presented a different behavior, the γ_s was of 25.09 mJ/m^2, and the dispersive component was γ_s^d= 20.07 mJ/m^2 and the polar component was γ_s^p = 5.02 mJ/m^2. A two times reduction of γ_s, and $\gamma_s^d > \gamma_s^p$ (~4 times) for S-OTMS particles, when compared to S-Na/SO_4 particles, confirming the chemical modification and the formation of a hydrophobic particle.

3.2.1. *Confocal fluorescence microscopic image*

Experiments using confocal laser scanning microscopy of the emulsions with the addition of S-Na/SO_4 particles suggested the Pickering effect, with particles organized at the interface (Fig. 5a-b), observed as a white layer of particles in these gray scale images (Fig. 5b). Silicone oil emulsions were indicated as black areas, and the castor oil continuous phase was stained with Nile blue fluorescent dye, associated with gray areas in the images.

The Pickering effect was observed in all formulations (Fig. 5a). The particles were aggregated at the droplet interface and also dispersed in the continuous phase. The S-Na/SO_4 emulsions formed a silicone-in-castor emulsion in the 0.3 and 0.5 fractions of silicone regardless of the particle concentration. However, when increasing the silicone fraction in the system (Φs = 0.7), a castor-in-silicone emulsion was formed. In this process, the increase of the silicon volume fraction formed castor-in-silicone emulsions. At higher concentrations of particles, a visible increase in the viscosity was observed by tilting the tube at 45°, and the emulsions produced were apparently stabilized due to the depletion effect observed. S-Na/SO_4 is a hydrophilic particle and should preferably form silicone-in-castor emulsions. Based on this, a possible explanation for the presence of multiple emulsions such as castor-in-silicone-in-castor (gray areas within the dispersed phase) could be that initially, silicone-in-castor emulsions were formed, and the rapid separation process of phases led to the formation of small stable droplets of castor in silicone.

In the cryo-TEM image (Fig. 6) obtained from the silicone-in-castor

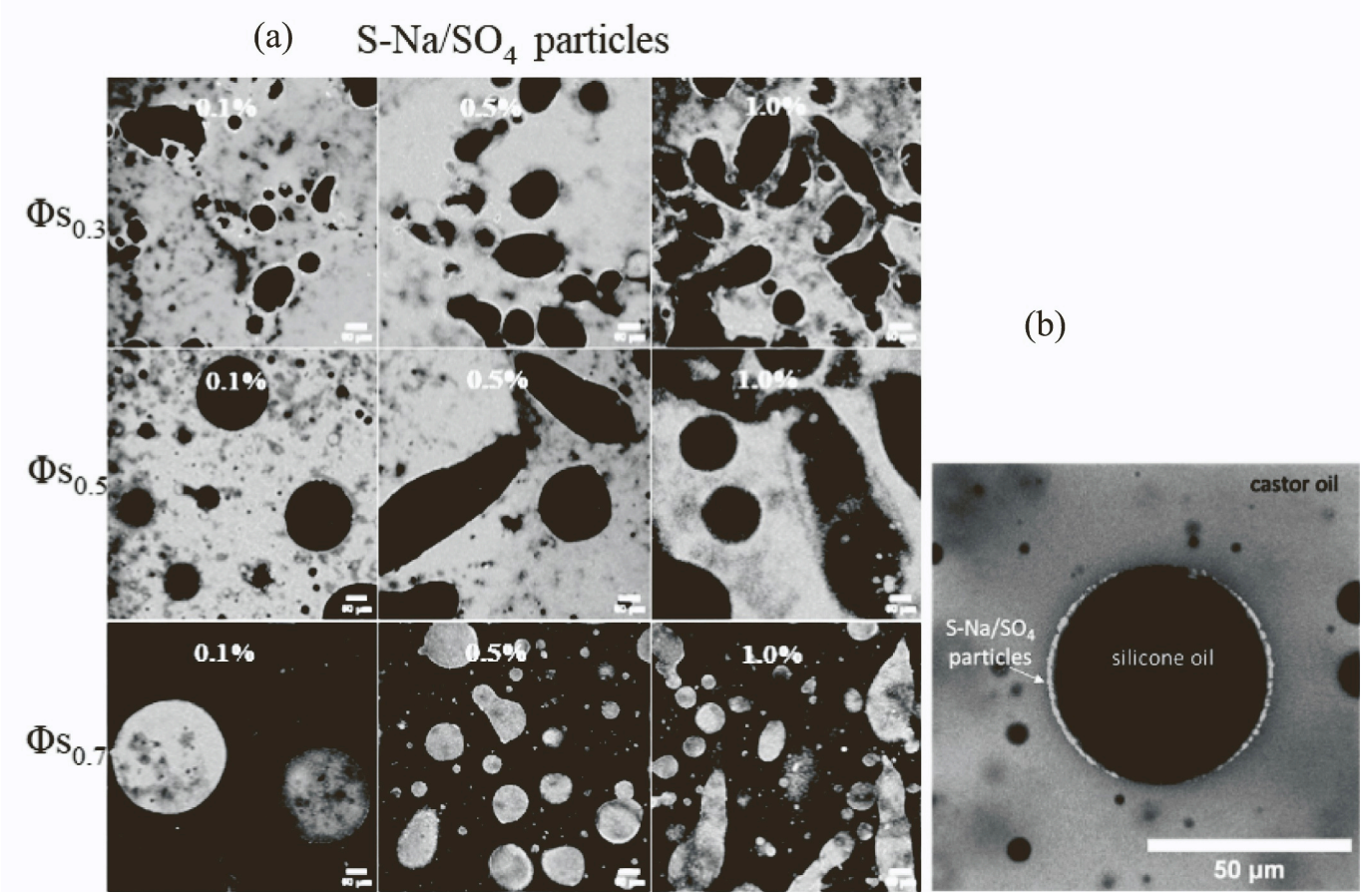

Fig. 5. (a) Confocal fluorescence microscopic image of emulsions containing silicone oil and castor oil (silicone oil fraction ranging from 0.3 to 0.7) and S-Na/SO_4 particles ranging from 0.10 to 1.0 wt% after preparation. 50 µm scale bar. (b) Closer view of one droplet of the emulsion containing silicone oil ($\Phi s_{0.3}$) and castor oil along with 1.0 wt% of S-Na/SO_4 particles after preparation.

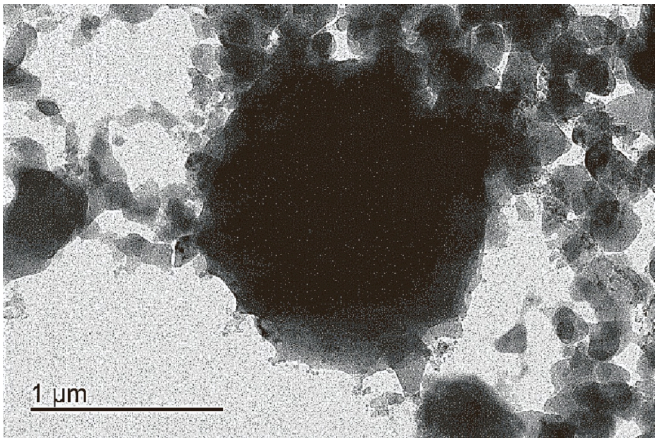

Fig. 6. Cryo-TEM image of a silicone-in-castor emulsion stabilized by 0.50 wt % S-Na/SO_4 particles and equal volumes of the two oils 24 h after preparation. Emulsion containing silicone oil ($\Phi_S = 0.5$).

oil emulsion stabilized by particles of S-Na/SO_4, two oil phases were distinguished from each other by their different coloration: castor oil is the light areas compared to the dark silicone oil. A small droplet can be seen in the TEM image (Fig. 6), with the particles arranged around the dark droplets (silicon oil). In addition, the smaller particles formed a network of interconnected particles in the continuous phase (castor oil), showing that hydrophilic particles of different sizes and shapes are effective in stabilizing oil-in-oil emulsions.

Using confocal fluorescence microscopy, spherical droplets of silicone with S-OTMS aggregates dispersed in this phase were also observed (Fig. 7a-b), indicating that most particles here were preferentially in the silicone phase than the castor oil phase.

The formulations containing the S-OTMS particles (Fig. 7a) showed silicone emulsions in castor oil at Φs of 0.3 and 0.5 and in the highest silicone compositions of the system (Φs of 0.7), there was phase inversion at all particle concentrations. However, there were bicontinuous regions, as in Φs of 0.5 with 1.0% by weight of particles, viewed microscopically in large mode (Fig. 7b), with a region containing silicone emulsions in castor oil and a region containing castor oil emulsion in silicone, in addition to particles dispersed in the silicone phase. Since the S-OTMS particles were grafted with octadecyltrimethoxysilane on the basal surfaces, hydrophobic particles were generated that partially interacted with/wetted the silicone phase, as observed in the measurements of the three-phase contact angle. Additionally, it was possible to create multiple emulsions in these bicontinuous systems.

The relationship between the rheology and the stability of these Pickering emulsions with hydrophilic and hydrophobic particles was systematically evaluated.

3.2.2. *Rheological study of emulsions*

The effect of S-Na/SO_4 and S-OTMS particles on the emulsions were studied by dynamic oscillatory rheology to measure the apparent viscosity and G' and G" moduli. The rheological response of the emulsion formulations was measured after 30 days of storage. Fig. 8 shows the apparent viscosity as a function of shear rates. Low viscosity of the pure oils (0.67 Pa.s for silicone oil and 0.57 Pa.s for castor oil) was observed over the entire shear range, but when dispersing S-Na/SO_4 (Fig. 8a) particles in silicone, the viscosity increased smoothly to 0.92 Pa.s, while in the system with castor oil, the viscosity was unaffected.

On the other hand, the emulsified system exhibited non-Newtonian behavior, with higher viscosity than pure liquids and a gradual decrease in the viscosity, and the absence of a plateau at low shear, suggesting the formation of permanent networks. Initially, the emulsion-S-Na/SO_4 system showed viscosity of 4.17 Pa.s and a shear thinning up to ~0.93 Pa.s, indicating that the emulsion droplet network was destroyed by shearing the sample, causing a decrease in viscosity. Compared with the emulsified system containing the S-OTMS particles (Fig. 8b), a small increase in apparent viscosity was observed at the very beginning of shearing (1.12 Pa.s), which decreased rapidly to 0.71 Pa.s.

The results presented in Fig. 9a show that the rheological properties of Pickering emulsions with S-Na/SO_4 particles evolved with increasing particle concentration. In all rheological curves, G' and G" increased in magnitude with increasing frequency applied, with G' being more significant than G", indicating that the emulsions presented elastic behavior, characteristic of solid viscoelastic fluids.

At the highest concentrations of S-Na/SO_4 particles (1.0% by weight), drastic changes in the droplet size distribution were observed (large and deformed droplets, as seen in Fig. 5). These changes particularly affected the rheology of the emulsion. Furthermore, the higher concentration of particles resulted in higher storage modulus and stronger elastic behavior.

This was because continuous phase particles can form a network structure, and the higher the concentration, the stronger the structure is, indicating high stability of the Pickering emulsion. The phase transition

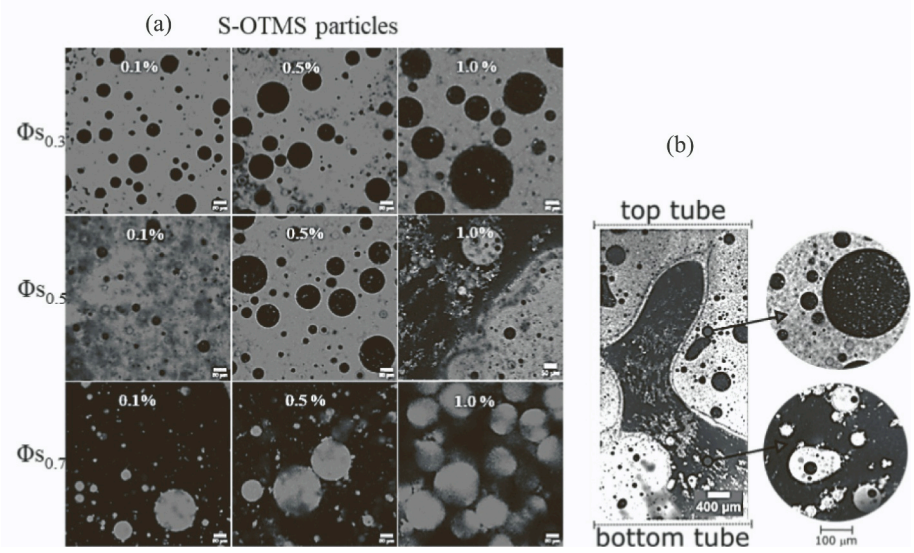

Fig. 7. (a) Confocal fluorescence microscopic image of emulsions containing silicone oil and castor oil (silicone oil fraction ranging from 0.3 to 0.7) and S-OTMS particles ranging from 0.1 to 1.0 wt% 24 h after preparation. The scale bar is 50 µm. (b) Total tube image (large mode).

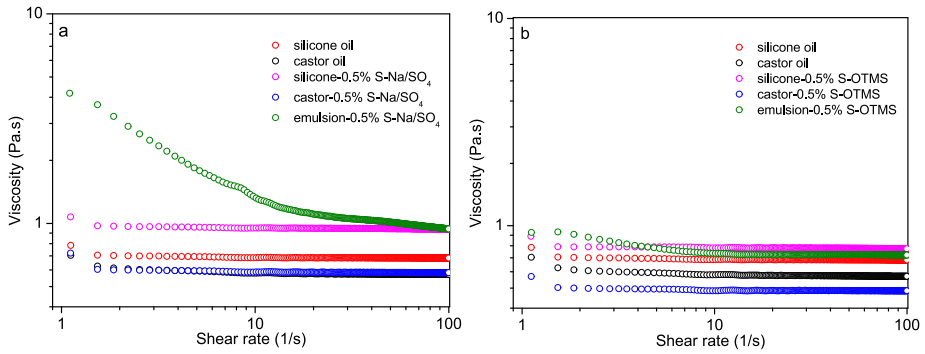

Fig. 8. Viscosity as a function of shear rate for samples: silicone oil, castor oil, particles dispersed in oils and emulsion (Φ_s of 0.5 and 0.5 wt% particles S-Na/SO_4 (A) or S-OTMS (B)).

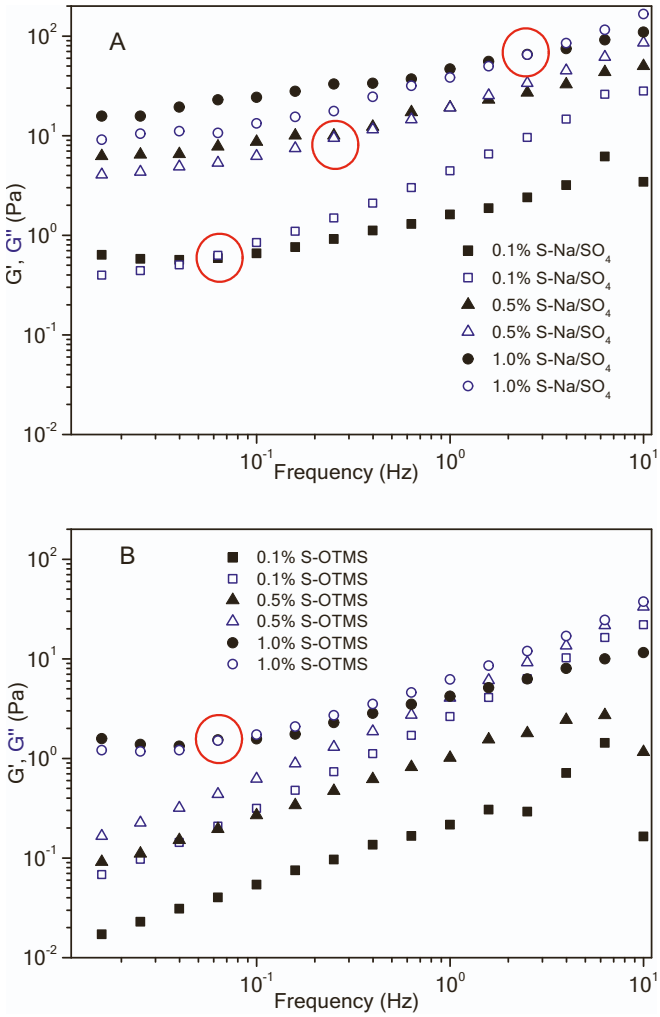

Fig. 9. Rheology data for emulsions containing silicone oil (Φ_S = 0.5) and stabilized with (a) S-Na/SO_4 and (b) S-OTMS at various concentrations: (■) square for 0.1 wt%, (▲) triangle for 0.5 wt%, (●) circle for 1.0 wt% and elastic modulus (G′, solid symbols) and viscous modulus (G″, open symbols) as a function of frequency (Hz). The oscillatory stress studies for the emulsions are shown in Fig. S3.

point (red circular area) appeared at high frequencies and is attributed to the structural rearrangement of the emulsion or flow (Matos et al., 2018; Xu et al., 2021). With S-OTMS particles (Fig. 9B), the transition point occurred at low frequency and only at the highest particle concentration (1.0 wt%).

In the Pickering emulsions stabilized with layered particles, higher particle contents improved the stability. The reason for this may be that particle-particle interactions and particle-liquid interactions were increased at higher concentrations, forming a network structure. This network was more evident for the S-Na/SO_4 formulation, suggesting that the rheological properties of this model emulsion were mainly determined by the emulsified phase and/or dispersed phase, since the droplet size and the interactions between the droplets were clearly of greater importance. This result was different than that of the S-OTMS formulation, which presented a weak network structure formed by spherical droplets. These considerations explain the sensitivity of rheological measurements to the observed changes in emulsion microstructure.

Thus, we demonstrated that easily synthesized S-Na/SO_4 and S-OTMS particles were able to stabilize oil-in-oil emulsions. In addition, the modification of shigaite-like LDH with OTMS resulted in a change in the solubility profile, with linear alkyl chains making them more dispersible in the silicone oil, which in turn defined the dispersed phase of the emulsion. This system can be used in cosmetic formulations, coatings and biomedical applications that are sensitive to the presence of water. For example, Binks and Tyowua (2016), revised the formulations with two immiscible oil phases, and found as lubricants on fibers, foam inhibitors, electro-reological fluids and display devices, personal care and cosmetics, vehicles for chemical reactions and pharmaceutical formulations.

4. Conclusion

A shigaite-like layered double hydroxide with the ideal formula $[Mn_6Al_3(OH)_{18}][(SO_4)_2Na]\cdot 12H_2O$ (S-Na/SO_4) was synthesized by co-precipitation with increasing pH, and the particle surfaces were grafted with octadecyltrimethoxysilane (S-OTMS), in an apolar medium. Oil-in-oil Pickering emulsions stabilized by layered double hydroxides were explored in terms of affinity, stability and morphology by confocal laser microscopy and rheology techniques. Two particles with different hydrophobicity were analyzed: S-Na/SO_4 (hydrophilic particle) and S-OTMS (hydrophobic particle) at different concentrations of particles and fractions of silicone in castor oil. The total emulsified volume was achieved with the S-Na/SO_4 particles, suggesting high stability for up to 30 days. The sensitivity of the rheological measurements indicated the formation of a weak gel for the S-Na/SO_4 formulation, that contributes considerably to emulsion stabilization, due to particle-particle and particle-liquid interactions, formed by deformed droplets and a weaker gel structure for S-OTMS and by spherical droplets for high concentrations of particles. Thus, the simplicity of synthesis of layered particles and preparation of oil-in-oil emulsions make them ideal for water-free applications and open a new interfacial area to explore.

CRediT authorship contribution statement

Lilian Fernanda Martins do Amaral: Formal analysis, Investigation, Writing – original draft. **Gabriela Siegel Aires:** Formal analysis. **Fernando Wypych:** Conceptualization, Methodology, Funding acquisition, Supervision, Writing – review & editing. **Rilton Alves de Freitas:** Conceptualization, Methodology, Funding acquisition, Supervision, Writing – review & editing.

Declaration of Competing Interest

The authors declare the following financial interests/personal relationships which may be considered as potential competing interests:

Fernando Wypych and Rilton Alves de Freitas report financial support was provided by National Council for Scientific and Technological Development, Coordination of Higher Education Personnel Improvement and Finep - Financiadora de estudos e projetos. Prof. Rilton Alves de Freitas and Fernando Wypych reports a relationship with Federal University of Parana that includes: employment. Fernando Wypych and Rilton Alves de Freitas has no patent pending. Lilian Fernanda Martins do Amaral reports Ph.D. scholarship from Coordination of Higher Education Personnel Improvement.

Data availability

No data was used for the research described in the article.

Acknowledgments

This study was financed by the Office to Coordinate Improvement of Higher Education Personnel (CAPES, Finance Code 001); National Council for Scientific and Technological Development (CNPq, FW Project 300988/2019-2; RAF Projects 301172/2016-1; 430451/2018-0; 303312/2019-0), and Financier or Studies and Projects (FINEP). LFMS acknowledges the Ph.D. scholarship from CAPES and we acknowledge the Center for Electron Microscopy of Federal University of Paraná (CME-UFPR) for the SEM measurements, the Center for Advanced Fluorescence Technologies (CTAF-UFPR) for the CLSM measurements, and Prof. Marco Tadeu Grassi for the ICP-OES analyses.

Appendix A. Supplementary data

Supplementary data to this article can be found online at https://doi.org/10.1016/j.clay.2023.106947.

References

Amaral, L.F.M., de Freitas, R.A., Wypych, F., 2020. K-shigaite-like layered double hydroxide particles as Pickering emulsifiers in oil/water emulsions. Appl. Clay Sci. 193, 105660 https://doi.org/10.1016/j.clay.2020.105660.

Amaral, L.F.M., Wypych, F., de Freitas, R.A., 2021. Shigaite, natroglaucocerinite and motukoreaite-like layered double hydroxides as Pickering emulsifiers in water/oil emulsions: a comparative study. Appl. Clay Sci. 201, 105918 https://doi.org/10.1016/j.clay.2020.105918.

Atanase, L.I., Riess, G., 2011. Block copolymers as polymeric stabilizers in non-aqueous emulsion polymerization. Polym. Int. 60, 1563–1573. https://doi.org/10.1002/pi.3137.

Bielas, R., Józefczak, A., 2020. The effect of Particle Shell on Cooling rates in Oil-in-Oil magnetic Pickering emulsions. Materials (Basel). 13, 4783. https://doi.org/10.3390/ma13214783.

Binks, B.P., Tyowua, A.T., 2016. Oil-in-oil emulsions stabilised solely by solid particles. Soft Matter 12, 876–887. https://doi.org/10.1039/C5SM02438B.

Carrasco, J.A., Seijas-Da Silva, A., Oestreicher, V., Romero, J., Márkus, B.G., Simon, F., Vieira, B.J.C., Waerenborgh, J.C., Abellán, G., Coronado, E., 2020. Fundamental Insights into the Covalent Silane Functionalization of NiFe Layered double Hydroxides. Chem. Eur. J. 26, 6504–6517. https://doi.org/10.1002/CHEM.201905397.

Chen, C., Yang, M., Wang, Q., Buffet, J.C., O'Hare, D., 2014. Synthesis and characterisation of aqueous miscible organic-layered double hydroxides. J. Mater. Chem. A 2, 15102–15110. https://doi.org/10.1039/C4TA02277G.

Chen, C., Buffet, J.C., O'Hare, D., 2020. Surface modification of aqueous miscible organic layered double hydroxides (AMO-LDHs). Dalton Trans. 49, 8498–8503. https://doi.org/10.1039/D0DT01213K.

Cooper, M.A., Hawthorne, F.C., 1996. The crystal structure of Shigaite, [$AlMn^{2+}_2(OH)_6]_3(SO_4)_2.Na(H_2O)_6(H_2O)_6$, a hydrotalcite-group mineral. Can. Mineral. 34, 91–97.

Crepaldi, E.L., Pavan, P.C., Valim, J.B., 1999. A new method of intercalation by anion exchange in layered double hydroxides. Chem. Commun. 155–156 https://doi.org/10.1039/A808567F.

Dyab, A.K.F., Mohamed, L.A., Taha, F., 2018. Non-aqueous olive oil-in-glycerin (o/o) Pickering emulsions: preparation, characterization and in vitro aspirin release. J. Dispers. Sci. Technol. 39, 890–900. https://doi.org/10.1080/01932691.2017.1406368.

Finkle, P., Draper, H.D., Hildebrand, J.H., 1923. The theory of emulsification. J. Amer. Chem. Soc. 45, 2780–2788.

Gomez, N.A.G., Sotiles, A.R., Wypych, F., 2020. Layered double hydroxides with the composition $[Mn_6Al_3(OH)_{18}][(HPO_4^{2-})_2A^+].yH2O$ (A^+= Li, Na or K) obtained by topotactic exchange reactions. Appl. Clay Sci. 193, 105658 https://doi.org/10.1016/j.clay.2020.105658.

Guo, W., Zhao, Y., Zhou, F., Yan, X., Fan, B., Li, R., 2016. Silylated layered double hydroxide nanosheets prepared by a large-scale synthesis method as hosts for intercalation of metal complexes. Appl. Catal. A Gen. 522, 101–108. https://doi.org/10.1016/J.APCATA.2016.05.001.

Klapper, M., Clark, C.G., Müllen, K., 2008. Application-directed syntheses of surface-functionalized organic and inorganic nanoparticles. Polym. Int. 57, 181–202. https://doi.org/10.1002/pi.2301.

Lisuzzo, L., Cavallaro, G., Milioto, S., Lazzara, G., 2022. Pickering emulsions stabilized by halloysite nanotubes: from general aspects to technological applications. Adv. Mater. Interfaces 9, 21023346. https://doi.org/10.1002/admi.202102346.

Matos, M., Laca, A., Rea, F., Iglesias, O., Rayner, M., Gutiérrez, G., 2018. O/W emulsions stabilized by OSA-modified starch granules versus non-ionic surfactant: Stability, rheological behaviour and resveratrol encapsulation. J. Food Eng. 222, 207–217. https://doi.org/10.1016/J.JFOODENG.2017.11.009.

Mei, Q., Luo, P., Zuo, Y., Li, J., Zou, Q., Li, Y., Jiang, D., Wang, Y., 2018. Formulation and in vitro characterization of rifampicin-loaded porous poly (ε-caprolactone) microspheres for sustained skeletal delivery. Drug Des. Devel. Ther. 12, 1533–1544. https://doi.org/10.2147/DDDT.S163005.

Owens, D.K., Wendt, R.C., 1969. Estimation of the surface free energy of polymers. J. Appl. Polym. Sci. 13, 1741–1747. https://doi.org/10.1002/app.1969.070130815.

Park, A.Y., Kwon, H., Woo, A.J., Kim, S.J., 2005. Layered double hydroxide surface modified with (3-aminopropyl) triethoxysilane by covalent bonding. Adv. Mater. 17, 106–109. https://doi.org/10.1002/ADMA.200400135.

Rodier, B., De Leon, A., Hemmingsen, C., Pentzer, E., 2017. Controlling oil-in-oil Pickering-type emulsions using 2D materials as surfactant. ACS Macro Lett. 6, 1201–1206. https://doi.org/10.1021/acsmacrolett.7b00648.

Rozynek, Z., Bielas, R., Jó, A., 2018. Efficient formation of oil-in-oil Pickering emulsions with narrow size distributions by using electric fields †. 5140 |. Soft Matter 14, 5140. https://doi.org/10.1039/c8sm00671g.

Sharma, T., Kumar, G.S., Chon, B.H., Sangwai, J.S., 2015. Thermal stability of oil-in-water Pickering emulsion in the presence of nanoparticle, surfactant, and polymer. J. Ind. Eng. Chem. 22, 324–334. https://doi.org/10.1016/J.JIEC.2014.07.026.

Sotiles, A.R., Wypych, F., 2019. Converting Mn/Al layered double hydroxide anion exchangers into cation exchangers by topotactic reactions using alkali metal sulfate solutions. Chem. Commun. 55, 7824–7827. https://doi.org/10.1039/c9cc03491a.

Sotiles, A.R., Wypych, F., 2020. First synthesis of a nanohybrid composed of a layered double hydroxide of Zn2Al intercalated with $SO_4^{2-}/Na^+/Ag^+$ and decorated with Ag^0 nanoparticles. J. Solid State Chem. 288, 121394 https://doi.org/10.1016/j.jssc.2020.121394.

Sotiles, A., Gomez, N., da Silva, S., Wypych, F., 2019. Layered double hydroxides with the composition Mn/Al-SO_4-A (A = Li, Na, K; Mn:Al ca. 1:1) as cation exchangers. J. Braz. Chem. Soc. 30, 1807–1813. https://doi.org/10.21577/0103-5053.20190087.

Sotiles, A.R., Baika, L.M., Grassi, M.T., Wypych, F., 2019a. Cation exchange reactions in layered double hydroxides intercalated with sulfate and alkaline cations $(A(H_2O)_6)[M_6^{2+}Al_3(OH)_{18}(SO_4)_2]\cdot 6H_2O$ (M^{2+} = Mn, Mg, Zn; A^+ = Li, Na, K). J. Am. Chem. Soc. 141, 531–540. https://doi.org/10.1021/jacs.8b11389.

Sotiles, A.R., Gomez, N.A.G., dos Santos, M.P., Grassi, M.T., Wypych, F., 2019b. Synthesis, characterization, thermal behavior and exchange reactions of new phases of layered double hydroxides with the chemical composition $[M_6^{+2}Al_3(OH)_{18}(SO_4)_2].(A(H_2O)_6).6H_2O$ (M^{+2} = Co, Ni; A = Li^+, Na^+, K^+). Appl. Clay Sci. 181, 1–10. https://doi.org/10.1016/j.clay.2019.105217.

Tadros, T.F., 2013. Emulsion Formation, Stability, and Rheology, Emulsion Formation and Stability. Wiley-VCH Verlag GmbH & Co. KGaA, Weinheim, Germany. https://doi.org/10.1002/9783527647941.ch1.

Tao, Q., He, H., Li, T., Frost, R.L., Zhang, D., He, Z., 2014. Tailoring surface properties and structure of layered double hydroxides using silanes with different number of functional groups. J. Solid State Chem. 213, 176–181. https://doi.org/10.1016/J.JSSC.2014.02.032.

Tawfeek, A.M., Dyab, A.K.F., Al-Lohedan, H.A., 2014. Synergetic effect of Reactive Surfactants and Clay Particles on Stabilization of Nonaqueous Oil-in-Oil (o/o) Emulsions. J. Dispers. Sci. Technol. 35, 265–272.

Thompson, K.L., Lane, J.A., Derry, M.J., Armes, S.P., 2015. Non-aqueous isorefractive Pickering emulsions. Langmuir 31, 4373–4376. https://doi.org/10.1021/acs.langmuir.5b00630.

Tyowua, A.T., Yiase, S.G., Binks, B.P., 2017. Double oil-in-oil-in-oil emulsions stabilised solely by particles. J. Colloid Interface Sci. 488, 127–134. https://doi.org/10.1016/j.jcis.2016.10.089.

Vaccari, A., 2002. Layered double hydroxides: present and futureV. Rives (Ed.), Nova Science Publishers, Inc., New York, 2001, IX+439 pp., ISBN 1-59033-060-9. Appl. Clay Sci. 22, 75–76. https://doi.org/10.1016/s0169-1317(02)00112-6.

Vartanian, R.D., Brook, B., 1969. Stable mineral oil-silicone oil compositions. United State Patent 2–4.

Wang, J., Stevens, L.A., Drage, T.C., Wood, J., 2012. Preparation and CO2 adsorption of amine modified Mg–Al LDH via exfoliation route. Chem. Eng. Sci. 68, 424–431. https://doi.org/10.1016/J.CES.2011.09.052.

Wang, S., Shen, Y., Chen, X., Dong, L., Yu, H., Bao, M., Li, Y., 2022. Cationic surfactant-modified palygorskite particles as effective stabilizaer for Pickering emulsion gel formation. Appl. Clay Sci. 219, 106439 https://doi.org/10.1016/j.clay.2022.106439.

Wypych, F., Satyanarayana, K.G., 2004. Interface Science and Technology. In: Interface Science and Technology. https://doi.org/10.1016/S1573-4285(13)70004-8.

Wypych, F., Bail, A., Halma, M., Nakagaki, S., 2005. Immobilization of iron(III) porphyrins on exfoliated MgAl layered double hydroxide, grafted with (3-aminopropyl)triethoxysilane. J. Catal. 234, 431–437. https://doi.org/10.1016/J.JCAT.2005.07.013.

Xu, W., Wang, S., Li, A., Wang, X., 2016. Synthesis of aminopropyltriethoxysilane grafted/tripolyphosphate intercalated ZnAl LDHs and their performance in the flame retardancy and smoke suppression of polyurethane elastomer. RSC Adv. 6, 48189–48198. https://doi.org/10.1039/C6RA06713A.

Xu, W., Zheng, S., Sun, H., Ning, Y., Jia, Y., Luo, D., Li, Y., Shah, B.R., 2021. Rheological behavior and microstructure of Pickering emulsions based on different concentrations of gliadin/sodium caseinate nanoparticles. Eur. Food Res. Technol. 247, 2621–2633. https://doi.org/10.1007/S00217-021-03827-6.

Yu, L., Li, S., Stubbs, L.P., Lau, H.C., 2021. Characterization of clay-stabilized, oil-in-water Pickering emulsion for potential conformance control in high-salinity, high temperatura reservoirs. Appl. Clay Sci. 213, 106246 https://doi.org/10.1016/j.clay.2021.106246.

Zhang, C., Yu, J., Xue, L., Sun, Y., 2017. Investigation of γ-(2,3-Epoxypropoxy) propyltrimethoxy silane surface modified layered double hydroxides improving UV ageing resistance of Asphalt. Mater. 2017 10, 78, 10, 78. https://doi.org/10.3390/MA10010078.

Zia, A., Pentzer, E., Thickett, S., Kempe, K., 2020. Advances and opportunities of oil-in-oil emulsions. Cite This ACS Appl. Mater. Interf. 12, 38861. https://doi.org/10.1021/acsami.0c07993.